Constrained optimal foraging by marine bacterioplankton on particulate organic matter

Yutaka Yawata[a,b,c,1,2], Francesco Carrara[a,1], Filippo Menolascina[d], and Roman Stocker[a,2]

[a]Department of Civil, Environmental and Geomatic Engineering, Institute of Environmental Engineering, ETH Zurich, 8093 Zurich, Switzerland; [b]Faculty of Life and Environmental Sciences, University of Tsukuba, 305-0001 Tsukuba, Japan; [c]Microbiology Research Center for Sustainability, University of Tsukuba, 305-0001 Tsukuba, Japan; and [d]School of Engineering, Institute for Bioengineering, The University of Edinburgh, EH9 3BF Edinburgh, United Kingdom

Edited by James H. Brown, University of New Mexico, Morro Bay, CA, and approved August 18, 2020 (received for review June 22, 2020)

Optimal foraging theory provides a framework to understand how organisms balance the benefits of harvesting resources within a patch with the sum of the metabolic, predation, and missed opportunity costs of foraging. Here, we show that, after accounting for the limited environmental information available to microorganisms, optimal foraging theory and, in particular, patch use theory also applies to the behavior of marine bacteria in particle seascapes. Combining modeling and experiments, we find that the marine bacterium *Vibrio ordalii* optimizes nutrient uptake by rapidly switching between attached and planktonic lifestyles, departing particles when their nutrient concentration is more than hundredfold higher than background. In accordance with predictions from patch use theory, single-cell tracking reveals that bacteria spend less time on nutrient-poor particles and on particles within environments that are rich or in which the travel time between particles is smaller, indicating that bacteria tune the nutrient concentration at detachment to increase their fitness. A mathematical model shows that the observed behavioral switching between exploitation and dispersal is consistent with foraging optimality under limited information, namely, the ability to assess the harvest rate of nutrients leaking from particles by molecular diffusion. This work demonstrates how fundamental principles in behavioral ecology traditionally applied to animals can hold right down to the scale of microorganisms and highlights the exquisite adaptations of marine bacterial foraging. The present study thus provides a blueprint for a mechanistic understanding of bacterial uptake of dissolved organic matter and bacterial production in the ocean—processes that are fundamental to the global carbon cycle.

patch use theory | *Vibrio* sp. | motility | biofilm | cyclic di-GMP

Heterotrophic bacteria are the primary recyclers of dissolved organic matter (DOM) in the ocean (1, 2). While numerically dominant groups of bacteria, such as *Pelagibacter*, rely on diffusion to take up DOM at the low nearly uniform concentrations that occur in the bulk of the ocean's water column, other groups—referred to as copiotrophs—display distinct behavioral adaptations to take advantage of microscale DOM hotspots (3–6). Particles, such as marine snow, represent an important example of such hotspots. Their importance stems from their role in the biological pump, the large flux of particulate carbon from surface waters to the deep ocean (1, 2, 7), which is mediated by particle degradation by diverse communities of heterotrophic bacteria (8). This microbial influence on the global carbon cycle is, thus, ultimately dependent on the ability of bacteria to find and take up nutrients from particles. Borrowing terminology from behavioral ecology, we refer to this process of searching for and exploiting particles as foraging (9, 10).

Resource foraging in heterogeneous landscapes is a classic paradigm in behavioral ecology (11). Birds (12–14) and insects (15, 16) actively balance the residence time within a resource patch and the search time for the next patch to optimize their individual fitness due to energy intake. The behavior most suited for a given resource landscape is predicted by optimal foraging theory (OFT) (11), which provides a predictive framework to study the trade-off between exploitation of a patch, predation risk, and dispersal to seek fresh patches. Because the marine landscape on the microscale is composed of discrete resource patches at time and length scales commensurate with bacterial dispersal (9), we hypothesized that the adaptations for nutrient acquisition of marine bacteria might be understood using the framework of patch use theory—one pillar of OFT together with diet choice and habitat selection—with particles as resource patches. These adaptations include, among others, two pervasive bacterial behaviors, motility and attachment to surfaces (17). These behaviors have been studied mostly in isolation, and although it is known that bacteria can switch from one to the other (18, 19), no theoretical framework exists to predict the relative performance of bacterial foraging strategies in a patchy environment.

Here, we show that marine bacteria can display dynamic foraging strategies in which they alternate between attachment to exploit particles and motility to seek fresh particles. Using the marine bacterium *Vibrio ordalii* as a model system, we measure the performance of this foraging strategy on model marine particles at varying nutrient content and particle concentration. Interpreting the observations through a mathematical model, we show that this dynamic foraging strategy increases the fitness of a cell: Timely detachment from a particle when this is providing diminishing nutrient returns permits bacteria an early search for a fresh particle. We show that cells stayed longer on particles of higher quality and in poor environments or when the search time

Significance

Patch use theory predicts that organisms foraging in a heterogeneous resource landscape balance their residence time on a patch yielding diminishing returns with the sum of the metabolic, predation, and opportunity costs of foraging. By combining single-cell tracking with mathematical modeling, we show that bacteria foraging on seascapes of organic particles switch between attached and planktonic lifestyles and tune the time spent on particles to increase individual fitness. As predicted by patch use theory, bacteria remain longer on particles of higher quality and in poor environments, or when search times for fresh particles are longer. These results show that patch use theory can be a valuable framework to understand not only animals, but also microorganisms, and ultimately their ecosystem-level consequences.

Author contributions: Y.Y., F.C., F.M., and R.S. designed research; Y.Y. and F.C. performed research; Y.Y. and F.C. contributed new reagents/analytic tools; Y.Y., F.C., and F.M. analyzed data; and Y.Y., F.C., and R.S. wrote the paper.

The authors declare no competing interest.

This article is a PNAS Direct Submission.

[1]Y.Y. and F.C. contributed equally to this work.

[2]To whom correspondence may be addressed. Email: yawata.yutaka.ga@u.tsukuba.ac.jp or romanstocker@ethz.ch.

This article contains supporting information online at https://www.pnas.org/lookup/suppl/doi:10.1073/pnas.2012443117/-/DCSupplemental.

First published September 24, 2020.

for fresh particles was longer, as predicted by patch use theory. A mathematical model predicts that this form of bacterial foraging affords a considerable growth advantage over foraging behaviors in which the time of detachment is not regulated according to particle quality and is robust over a wide range of particle concentrations typical of coastal seawaters.

Results

Bacteria Switch between Sessile and Planktonic Lifestyles. Visualization of the marine bacterium *V. ordalii* 12B09 (20) exposed to model marine particles revealed that cells rapidly switch between sessile and planktonic lifestyles (Fig. 1 *A* and *B*, Fig. S1*A*, Movie S1, and Dataset S1). As a simplified model of marine particles (21), we used 500-μm agarose spheres loaded with tryptone and gently added these to a suspension of green fluorescent protein (GFP)-tagged *V. ordalii*. Epifluorescent imaging revealed rapid colonization of the particles on timescales of 1 to 2 min (Fig. 1 *A* and *B* and Fig. S1 *A* and *B*). The colonization is driven by chemotactic motility: As tryptone diffuses from the particles, it forms a gradient around them in a manner reminiscent of the diffusion of DOM from marine particles, and the tryptone gradients attract *V. ordalii*. Separate microfluidic experiments confirmed that *V. ordalii* is chemotactic toward tryptone (Fig. S1*C*).

Hotspots of DOM in the ocean, however, dissipate and are replaced by the appearance of new ones. In our system, agarose particles run out of tryptone as this diffuses into the surroundings (Fig. S1*D*). To mimic particle turnover, we added four to five particles to the bacterial suspension at regular (25-min) time intervals. Epifluorescence video microscopy revealed that bacteria selectively colonized the freshest particles (Fig. 1 *A* and *B*). The colonization of each particle was transient, and bacteria detached and moved back into the surrounding medium within ~5 min after colonization. This resulted in a highly dynamic sequence of colonization and departure events reflecting the origin and dissipation of new particles.

Attachment Response Is Regulated by Nutrient Dynamics. Surface attachment by *V. ordalii* is strongly dependent on nutrient concentration (Fig. 1*C* and Fig. S2*A*). Exposure to nutrients elicited the transition from planktonic to sessile in less than 2 min (Fig. S2*B*), and attachment was highly reversible, whereby sequential addition and removal of the nutrient led to a repeated attachment and detachment response (Fig. S2*C*). Addition of an inhibitor of diguanylate cyclase, the enzyme that catalyzes the formation of cyclic-di-GMP, attenuated the transition from planktonic to sessile (Fig. S3). Cyclic-di-GMP is an intracellular signaling molecule that regulates the loss of motility and initiation of surface attachment in the early stages of biofilm formation (18). This suggests that a regulatory circuit involving intracellular cyclic-di-GMP concentration is the likely molecular mechanism for the rapid phenotypic switch between sessile and planktonic phases of *V. ordalii*.

The nutrient-regulated attachment response was exhibited by a significant fraction of cells within *V. ordalii* populations and occurred under a broad range of environmental conditions. Experiments under a constant tryptone concentration showed that the number of cells that become surface attached is on the order of 10^3 mm^{-2} for the conditions tested (*Materials and Methods*). This value is comparable to that exhibited by another marine strain, *Vibrio cyclitrophicus* ZF270 (Fig. S4*A*), known to be an ecotype that readily attaches and forms biofilms (but which, in contrast, does not exhibit detachment when nutrients dwindle; Fig. S2*C*). Induction of the attachment response by increased nutrient concentration in *V. ordalii* occurred under a wide range of pH values (pH = 5–10.5) and surface chemical properties

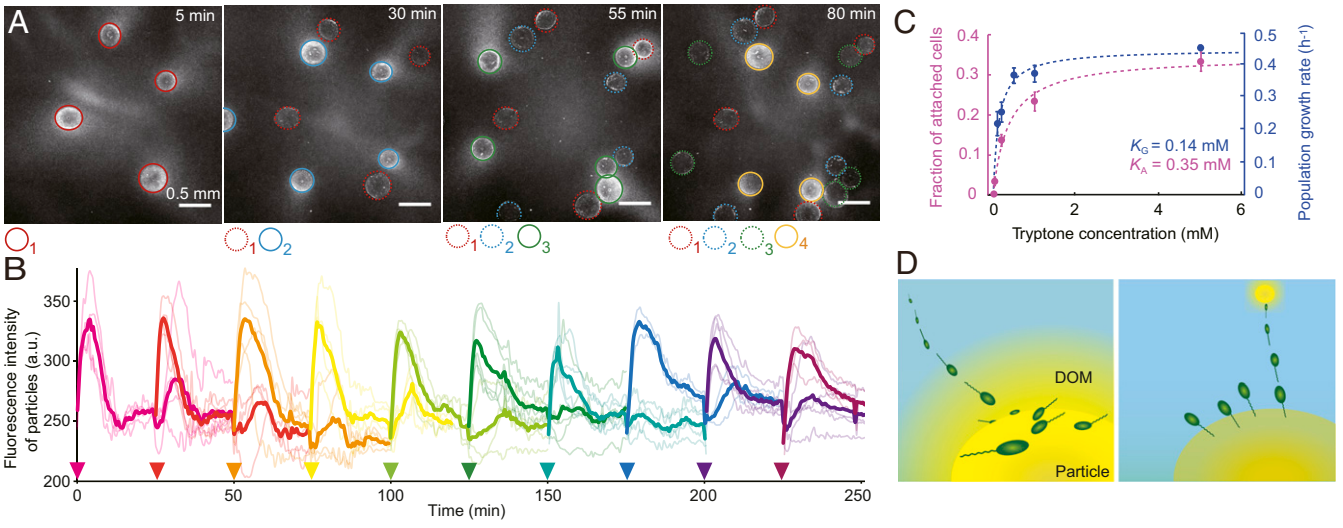

Fig. 1. *V. ordalii* exhibits a highly dynamic foraging strategy, rapidly attaching to fresh nutrient particles, and detaching from spent ones. (*A*) Micrographs showing colonization and decolonization of particles. Particles are color coded according to the order in which they were added (at 25-min intervals starting at t = 0; see legend below the panel). Solid outlines indicate newly added particles, and dotted outlines indicate those added at previous time points. Fluorescent bacteria appear as bright pixels on a dark background. (*B*) Time course of fluorescence intensity (a.u.) of newly added particles. The average intensity (thick lines) is shown for sets of individual particles (thin lines) added at the same time point. Lines and triangles (time points of addition) are color coded according to the consecutive additions of particles. (*C*) *V. ordalii*'s attachment to surfaces (left axis, purple) depends on the local concentration of tryptone. The fraction of cells adhering to a test surface (the lower surface of a plastic dish) was measured at equilibrium after 1 h of incubation in solutions of different tryptone concentrations. Circles show the average, and bars show the SD of three replicates. The dashed curve shows the fit with a Michaelis–Menten equation (K_A = 0.35 ± 0.08 mM). Population growth rate of *V. ordalii* in artificial seawater supplemented with different concentrations of tryptone (right axis, blue). Circles show the average and bars show the SD of three replicates. The dashed curve shows the fit with a Michaelis–Menten equation (K_G = 0.14 ± 0.02 mM). (*D*) Schematic of the dynamic foraging strategy used by *V. ordalii*. Bacteria locate particles, which are rich in DOM, by performing chemotaxis (*Left*). The high local DOM concentration rapidly induces cellular surface adhesiveness, and, once attached, cells take up DOM diffusing from the particle surface. As the DOM concentration declines, cellular adhesiveness decreases, and cells detach from the surface to initiate the search for fresh particles (*Right*).

ranging from hydrophilic to more hydrophobic (contact angle = 28°–79°) (Fig. S4 *B–D*).

The attachment kinetics of *V. ordalii* are tuned to efficiently exploit nutrients diffusing from the surface of marine particles. Experiments with different tryptone concentrations showed that the dependence of both attachment and growth kinetics on concentration, each described by a Michaelis–Menten function (Fig. 1*C*), have half-saturation constants of the same magnitude (attachment constant $K_A = 0.35 \pm 0.08$ mM; growth constant $K_G = 0.14 \pm 0.02$ mM; Fig. 1*C*). Taken together, our observations indicate that bacteria possess the ability, likely obtained through evolution, to detach from a surface when the nutrient released from it is no longer supporting a high growth rate. They achieve this by sensing the dwindling tryptone concentration at the particle surface by means of their surface chemoreceptors (22), rapidly shut down the attachment phenotype, and turn on the dispersal phenotype to swim into bulk seawater (Fig. 1 and Figs. S1 and S2). This phenotypic plasticity in surface attachment results in a foraging strategy in which cells selectively colonize resource-rich particles, which afford a high growth rate, then swiftly leave as the resource concentration on the particle fades in order to search for a fresh particle in the water column (Fig. 1*D*).

Bacterial Foraging Follows Predictions of Patch Use Theory. Bacteria leave a particle well before the nutrients on it are completely depleted and stay longer on a rich than on a poor particle as predicted by patch use theory. To determine the tryptone concentration at which each bacterium detached from the surface, hereafter referred to as the giving-up density (GUD), we designed a two-dimensional (2D) version of the experiment in which *V. ordalii* were exposed to a disk-shaped agarose patch initially loaded with tryptone. In this experimental arena, tryptone was the sole carbon, nitrogen, and phosphate source as cells were suspended in unsupplemented artificial seawater. This 2D system allowed the attachment and detachment of single bacteria to be monitored by time-lapse microscopy (Movie S2 and Dataset S2; it also revealed that *V. ordalii* attached at random locations on the surface and did not form spatial aggregates; Fig. S5). Experiments were performed at three different initial tryptone concentrations (0.2, 1.0, and 5.0 mM), hereafter referred to as the initial prey density (IPD). As in the case of the spherical model particles, the number of cells attached to the patch increased over time to a peak, then decreased as cells detached and returned into the surrounding liquid (Fig. 2 *B* and *C*). A quantification of the distribution of residence times of individual bacteria on the patch from the time-lapse images (Fig. 2*D*) revealed that the resident time was dependent on the IPD. The mean residence time was higher on higher-quality patches, with 35 min for the patch with IPD = 0.2 mM, 49 min for IPD = 1 mM, and 81 min for IPD = 5 mM. The diffusion of tryptone from the patch into the surroundings was quantified through a mathematical model (Fig. 2*A*), which also yielded the time course of the tryptone concentration at the patch surface $C(t)$ as it decreased through time due to molecular diffusion (Fig. 2*C* and Fig. S6 and *SI Appendix*). Bacterial uptake was not included in the analysis, based on additional simulations that showed it to be negligible in our experiments (Fig. S7 and *SI Appendix*). Combining these results, we obtained a curve for the detachment probability as a function of the tryptone concentration on the patch surface for each patch quality (i.e., initial tryptone concentration; Fig. 2*E*). We define the GUD as the tryptone concentration on the patch surface at which the number of attached bacteria dropped to 50% of the maximum number (Fig. 2*E*). Surprisingly, this analysis reveals a positive correlation between the initial patch quality and the concentration at which cells left the patch. The detachment concentration was 0.03 mM for the patch with IPD = 0.2 mM, 0.09 mM for IPD = 1 mM, and 0.36 mM for IPD = 5 mM—more than ten times higher for the highest-quality patch (IPD = 5 mM) compared to the lowest-quality patch (IPD = 0.2 mM), indicating that cells regulate the detachment threshold concentration in response to the IPD (Fig. 2*E*). Moreover, these detachment concentrations are on the order of 10–1000 μM across the three patch qualities (Fig. 2*E*), 20-fold greater than the background in the experiments at the time of detachment (Fig. S7 and *SI Appendix*), and up to 1,000-fold greater than typical background concentrations C_b of labile dissolved organic matter in the ocean ($C_b < 1$ μM, ref. 23). This suggests that *V. ordalii* cells spontaneously detach from a patch that is up to three orders of magnitude richer in nutrient concentration than the concentration in the surrounding seawater.

Further experiments were performed to determine the effect of the quality of the environment on the residence time of bacteria on particles in order to test a fundamental prediction of patch use theory, that residence time on a patch should decrease with increasing quality of the environment. In these experiments, bacteria were first allowed to attach to the surface of a glass Petri dish for 30 min at one of three tryptone concentrations (IPD = 0.2, 1, and 5 mM) and subsequently exposed to a smaller tryptone concentration *C* (Fig. S8). Monitoring the number of attached bacteria over time revealed that bacteria, indeed, remain attached for longer when the environment is poorer (IPD = 0.2 mM; Fig. S8*C*) than when it is richer (IPD = 1 mM; Fig. S8*B*) with the smallest residence time occurring in the richest environment (IPD = 5 mM; Fig. S8*A*). Furthermore, we quantified the proportion of cells remaining attached after 120 min as a function of the ratio *C*/IPD (Fig. 3*A*). This analysis indicates that bacteria do not have an intrinsic set point (i.e., concentration) at which they leave the surface but rather their residence time is set by the decrease in the nutrient concentration relatively to the reference environment (*C*/IPD). This emergent rescaling of the nutrient concentration at which cells detach aligns with the observation that cells appear to rescale their GUD by the IPD in the agarose disk setup (Fig. 2*E*).

V. ordalii increases its residence time in response to an increase in the search time. We mimicked a long search time by incubating cells for 3 h under starvation conditions in particle-free seawater. After starvation, bacteria were again first allowed to attach to the surface of a glass Petri dish for 30 min while exposed to 5 mM tryptone (the IPD) and subsequently exposed to a smaller tryptone concentration *C*. In these experiments, we compared the detachment behavior with that of a control population that had not experienced a long search time (Fig. 3*B*). Both populations adjusted their detachment probability according to the tryptone concentration *C*, but the behavior was not the same in starved cells and in the control population. Rather, the starved population had a higher proportion of cells remaining attached after 90 min at the lower concentrations of tryptone (*C* = 0, 0.1, and 0.2 mM). Although starvation is only a proxy for a long search time, these results suggest that cells adjust their residence time in response to the search time. We speculate that the reported increase in the residence time is mediated by metabolic changes occurring within the cell upon starvation, as suggested by the progressive loss of motility under starvation conditions (Fig. S9), rather than by a direct assessment of the opportunity costs associated with foraging.

Bacterial Foraging in Heterogeneous Nutrient Seascapes. In a heterogeneous resource seascape, as coastal seawater often is for heterotrophic bacteria, the benefit that would be gained from remaining attached to a particle as its resources dwindle is eventually balanced by the benefit that could be gained by seeking and finding a fresh particle—the opportunity cost—where this benefit is discounted by the lack of resource gain during the search time. The central prediction of patch use theory is that an organism should leave a patch when the harvest rate no longer balances the sum of metabolic, predation, and

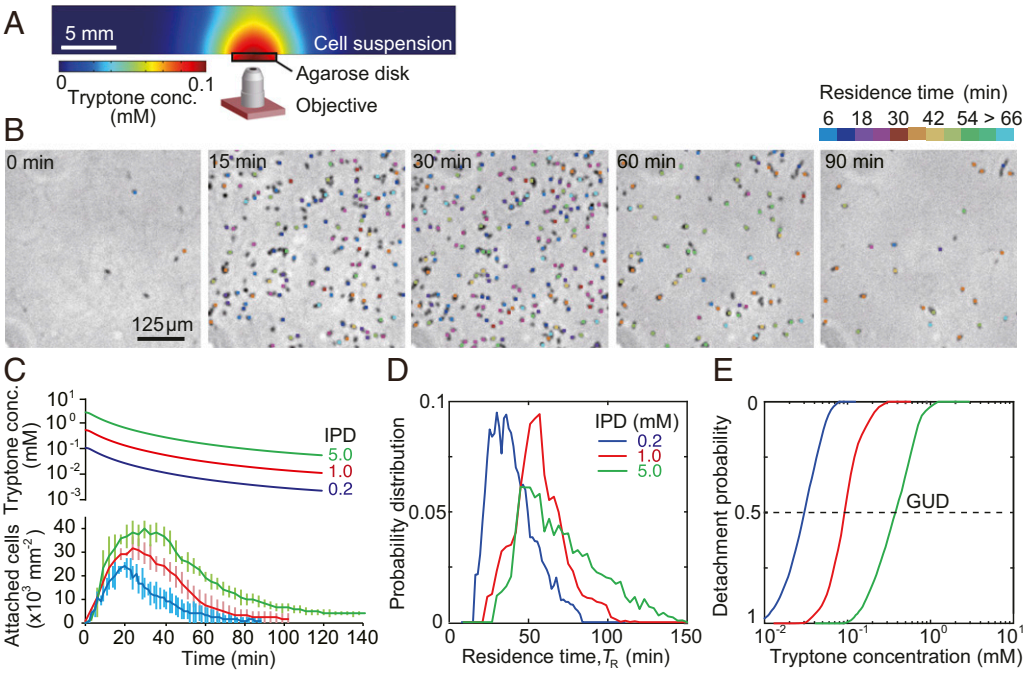

Fig. 2. *V. ordalii* fine-tunes the detachment time from the surface of a patch according to patch quality. (*A*) Illustration (side view) of the experimental arena used to quantify the residence time of individual bacteria on patches. A tryptone-loaded agarose disk (patch; 3.8-mm diameterand 0.5-mm thick) was used as a model of a particle, and a bacterial suspension in artificial seawater was introduced into the well containing the patch. The attachment and detachment times of individual bacteria at the patch surface were quantified from video recordings using a 20× objective as tryptone diffused out from the patch into the surrounding seawater. Colors show the tryptone concentration at $t = 30$ min as obtained from a numerical simulation of tryptone diffusion for a patch loaded with 1-mM tryptone (*SI Appendix*). (*B*) Time series of micrographs showing cells on the surface of the patch loaded with 1-mM tryptone. Cells are color coded according to their residence time T_R. (*C*) Time series of the concentration of tryptone at the patch surface, obtained from the numerical model (upper curves) and time series of the number of cells attached to the patch (lower curves), measured from the video recordings and color coded according to the initial tryptone concentration (IPD = 5, 1, or 0.2 mM). Lines show the SD of three replicates. (*D*) Probability distribution of the bacterial residence time on patches T_R, color coded according to the initial tryptone concentration. (*E*) Detachment probability as a function of the tryptone concentration at the patch surface, color coded according to the initial tryptone concentration. The black dashed line denotes the giving up density (GUD), the point at which half of the cells have detached from the patch.

opportunity costs of foraging. In this way, the organism will maximize its individual fitness. To quantitatively test the predictions from patch use theory for *V. ordalii*, we analyzed, with a mathematical model, how the timing of detachment would affect the nutrient uptake in the ocean. A bacterium foraging in a landscape of particles will maximize its time-averaged nutrient uptake when it detaches from its current particle and initiates the search for a new particle at the time point when the instantaneous uptake rate $U(t)$ declines to the same value as the time-averaged uptake rate, $U_m = \int_{T_0}^{T_i} U(t)\ \ dt/[\tau_s + T_R]$, where T_0 is the time at which the bacterium attached to the particle, T_i is the

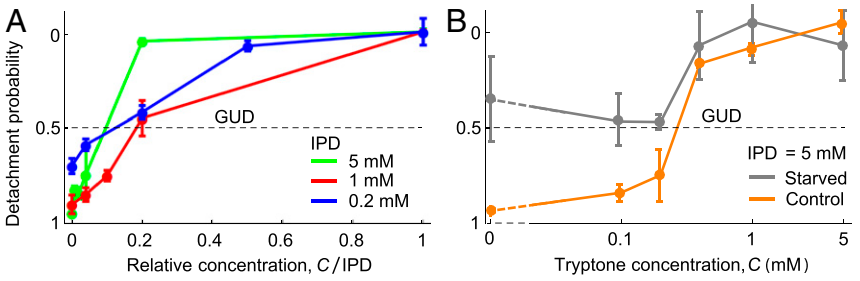

Fig. 3. *V. ordalii* adjusts its residence times on the surface of a patch depending on the environmental quality and the search time. (*A*) Detachment probability (measured in terms of the proportion of cells remaining attached) is governed by the relative magnitude of the nutrient concentration decrease of the patch compared to the environment. Bacteria were allowed to attach to the surface of a glass Petri dish for 30 min under an initial concentration IPD = 0.2, 1, and 5 mM of tryptone, then, the tryptone concentration was decreased to a value *C*, and the number of cells remaining attached after 120 min was quantified. Same data as in Fig. S8, shown for one single time point (120 min) as a function of the relative nutrient concentration *C*/IPD. Lower values of *C*/IPD denote a larger decrease in nutrient concentration. The black dashed line denotes the giving up density (GUD), the point at which half of the cells have detached from the patch (GUD). Symbols show the mean and SD of six replicate experiments. (*B*) Effect of search time in nutrient-depleted bulk seawater (i.e., starvation time) on detachment. Upon starvation, which can be considered a proxy for longer search times, a population decreases the detachment probability. To mimic a long search time, one batch of cells was incubated for 3 h in unsupplemented seawater (gray circles; starved) prior to being exposed to concentration IPD, whereas control cells (orange circles) were exposed to concentration IPD immediately after harvesting from preculture. Cells that were previously starved showed a longer residence time when exposed to the lower concentrations of tryptone ($C = 0$, 0.1, and 0.2 mM) compared to control cells. Cells were allowed to attach to the surface of a glass Petri dish for 30 min under an initial concentration IPD = 5 mM of tryptone. The concentration of tryptone was then decreased to a value *C*, and the number of cells remaining attached after 90 min was quantified. Symbols show the mean and SD of three replicates.

time at which it detaches, $T_R = T_i - T_0$ is the residence time on the particle, and τ_s is the average search time determined by migration until a new particle is encountered (Fig. S10 and *SI Appendix*). The search time depends on the bacterial dispersal rate (often expressed as an effective diffusivity resulting from motility, ref. 24), the particle size, sinking speed, and the particle concentration (24). Therefore, depending on environmental conditions in the ocean, the search time for a bacterium to find a particle can range from tens of minutes in phytoplankton-bloom-collapse conditions in coastal seawaters to several hours or even days in oligotrophic conditions in the open ocean (25, 26) (*SI Appendix*). The prescient optimal forager—one with perfect information of the current patch value and the distribution of patch types and travel times within the environment—would maximize the time-averaged nutrient uptake by accordingly adjusting its residence time T_R on a particle when the search time changes (11).

Classic optimal foraging theory requires that organisms possess information on the distance between patches—something that butterflies and birds can readily acquire (14, 27), but which is beyond the sensory capabilities of bacteria, which are limited to measurements of local concentration and gradients of dissolved compounds (9). In order to account for the lack of information available to bacteria regarding the particle concentration, we used a mathematical model to compare the time-averaged nutrient uptake of *V. ordalii* accounting for its foraging under imperfect information with that of a prescient forager. In these simulations, we quantified the time-averaged uptake rate for the two strategies in environments with different particle concentrations—i.e., different search times—and different patch qualities (different IPDs). Borrowing a concept from patch use theory for animals (28), we computed the relative foraging efficiency R_E (*SI Appendix*), a metric of how much the performance of *V. ordalii* falls short of that of a prescient forager. This analysis showed that the residence times of *V. ordalii* observed in our experiments (Fig. 2*D*) correspond to a very high relative foraging efficiency under a wide range of particle concentrations and qualities expected to occur in the coastal ocean. For the three different values of IPDs considered in our experiments (Fig. 2), R_E was found to be greater than 95% for all search times between 20 and 100 min and greater than 75% for all search times shorter than 6 h, meaning that R_E is rather insensitive to the search time (Figs. 4 *A*–*C* and 5*A*).

Our analysis suggests that *V. ordalii*, despite being able to increase its residence time under long starvation conditions ($\tau_s = 3$ h, Fig. 3*B*), has little or no necessity to precisely adjust its residence time on a particle in response to variation in the search time. Our model revealed the relative foraging efficiency R_E to be high and rather insensitive to variations at small values of the search time ($\tau_s < 3$ h)—that is, variations in particle concentration under rich conditions (Fig. 5*A*). We computed a foraging optimality index F, defined as the average efficiency R_E over a range of search times. The maximum of the foraging optimality index F_{max} over all possible residence times represents the optimal foraging strategy of a marine bacterium when the particle concentration (and, thus, the search time) is unpredictable. Based on the experimental observations of the residence time (Fig. 2*D*), we find that the foraging optimality index for *V. ordalii* is close to the maximum ($F > 90\%$ of F_{max}) for the three patch qualities examined ($F/F_{max} = 92\%$, 93%, and 95% for IPD = 0.2, 1, and 5 mM, respectively; colored points in Fig. 4 *D*–*F*). We considered 6 h as an upper limit of the search time in these analyses but conducted an additional analysis by increasing the upper limit to 24 h to confirm the insensitivity of the results to the particular choice of the range of search times (Fig. S11). We propose to call this a constrained optimal foraging strategy to reflect the near-optimal foraging performance in the face of the constraints on bacterial sensory capabilities.

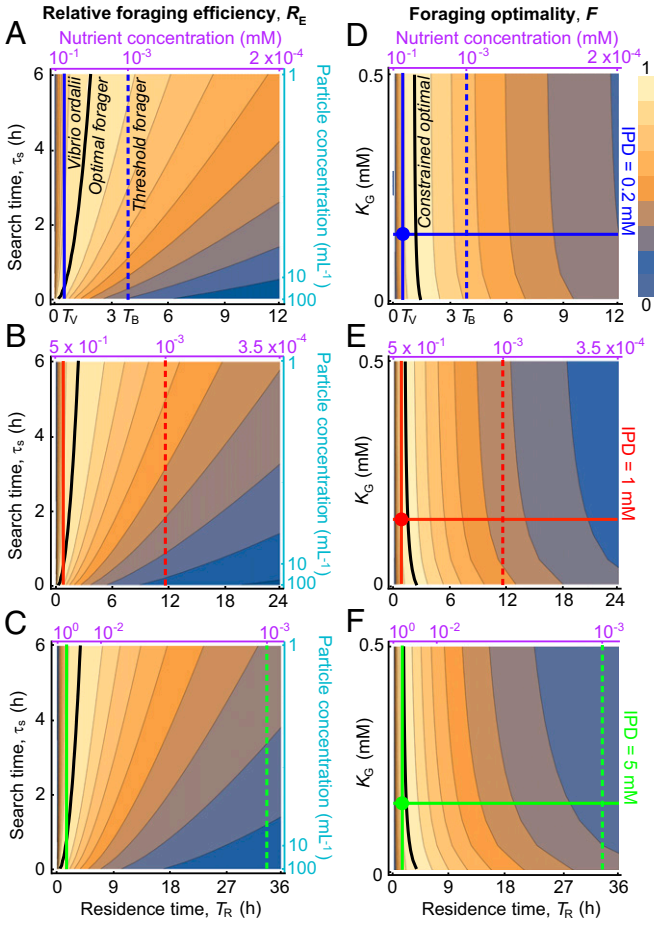

Fig. 4. *V. ordalii*'s foraging efficiency is high across a broad range of particle concentrations. (*A*–*C*) Relative foraging efficiency R_E (color coded) as a function of search time (left axis) (i.e., particle concentration in the ocean; right axis) and residence time on the particle (lower axis) (i.e., nutrient concentration of the particle at the moment of departure; upper axis) for low (IPD = 0.2-mM tryptone, *A*), intermediate (IPD = 1-mM tryptone, *B*), and high (IPD = 5-mM tryptone, *C*) patch qualities. Solid colored lines indicate the mean residence time of a population of cells in our experiments T_V (Fig. 2*D*). Dashed colored lines represent a fixed-threshold strategy T_B in which bacteria leave the particle at a concentration of 1 μM. Thick black lines indicate the foraging efficiency of the optimal forager (which regulates residence time as a function of search time). (*D*–*F*) Foraging optimality index F (color coded) as a function of the half-saturation constant for growth K_G and the residence time on the particle (lower axis) (i.e., nutrient concentration of the particle at the moment of departure; upper axis) for low (*D*), intermediate (*E*), and high (*F*) patch qualities. Empirically measured values of K_G (Fig. 1*C*) and residence time T_V (Fig. 2*D*) are indicated by horizontal and vertical solid colored lines, respectively. Colored circles represent the measured values of T_R and K_G, averaged over three replicates. Dashed colored lines represent a fixed-threshold strategy T_B in which bacteria leave the particle at a concentration of 1 μM. Thick black lines indicate the constrained optimal foraging strategy for different growth kinetics (i.e., K_G). *V. ordalii* actively swim for up to 6 h in seawater after which the proportion of swimming cells sharply decays (Fig. S9). We thus considered 6 h as an upper limit to the search time but tested the sensitivity of the results by varying the upper limit of the search time up to 24 h (Fig. S11).

By appropriately tuning its residence time on particles of different qualities, *V. ordalii* increases its fitness compared to other possible foraging strategies in the ocean. Two alternative strategies that would be physiologically simple to implement would be for bacteria to detach from a particle: (i) at a fixed threshold GUD = C_b where $C_b = 1$ μM is the background concentration of total amino acids in the bulk seawater, or (ii) after a random

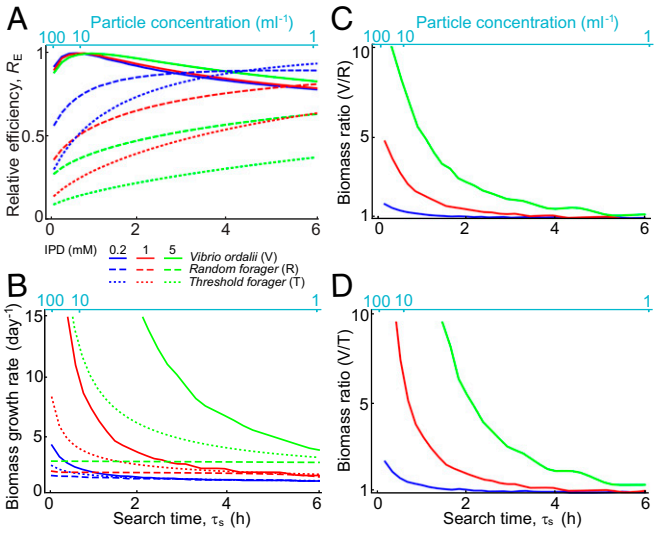

Fig. 5. *Vibrio ordalii*'s foraging strategy is most efficient in rich environments. (*A*) Relative foraging efficiency R_E as a function of search time τ_s (lower axis) (i.e., particle concentration in the ocean; upper axis), predicted by a mathematical model for different foraging strategies (*SI Appendix*): The constrained optimal foraging of *V. ordalii* (solid curves; symbol "V"; measured along the transect shown by vertical solid lines in Fig. 4 *A–C*); detachment from the particle at random times (dashed curves; symbol "R"); and detachment from the particle at a fixed nutrient concentration threshold of 1 μM (dotted curves; symbol "T"). Curves are color coded according to patch quality (represented by tryptone concentration in our experiments). (*B*) Biomass growth rate for the foraging strategies shown in *A*. (*C* and *D*) Ratio of biomass growth rate of a constrained optimal forager relative to (*C*) a random detacher and (*D*) a 1-μM-threshold detacher.

amount of time (*SI Appendix*) as has previously been assumed by modeling bacteria—particle interactions as a stochastic process (29, 30). Our results suggest that, for both of these strategies, the average uptake rate is reduced compared to the observed constrained optimal foraging of *V. ordalii*, particularly, at high particle concentrations (or, equivalently, at lower search times, Figs. 4 and 5). Accounting for the growth kinetics of *V. ordalii* (Fig. 1*C*), these alternative strategies would result in a biomass production over one day that is up to 10-fold lower than that achieved through constrained optimal foraging at the high end of the spectrum of particle concentrations (*SI Appendix* and Fig. 5 *B–D*), highlighting the great advantage gained through the nutrient-dependent dynamic switching between attached and planktonic lifestyles in *V. ordalii.*

Discussion

While it has been known for some time that marine bacteria possess a diverse repertoire of metabolic processes (31), it is only now beginning to emerge that they also possess a repertoire of exquisite behavioral strategies (32) that belie their apparent simplicity and contribute to fine-scale ecological differentiation and species coexistence. Previous studies have argued that a fundamental differentiation in foraging strategies exists among marine bacteria that either irreversibly attach to particle surfaces or remain planktonic in a fugitive strategy (8), such as the lineages of *V. cyclitrophicus* that are specialized into either sessile biofilm-forming or planktonic dispersing lifestyles in a competition—dispersal tradeoff that enables their coexistence (17). In contrast, the foraging strategy of *V. ordalii* described here involves rapidly and repeatedly switching between sessile and planktonic lifestyles in a manner that we suggest optimizes their resource gain. In light of the above observations, we propose that foraging strategies among marine bacterioplankton should be considered as forming a behavioral continuum rather than being characterized by a simple dichotomy of sessile and planktonic lifestyles. This view as a continuum should also encompass biofilm-forming species (33) and bacterial species displaying swarming motility (34), archetypes of a sessile lifestyle but which are, in fact, capable of spontaneously degrading the extracellular matrix and dispersing into the surroundings (19) in what may be a mechanism to allow cells to migrate and colonize new habitats (18).

We believe that the type of behavioral data obtained from our experimental setup where the nutrient concentration is a decreasing function of time (a "dynamic surface") is, per se, a novelty in the field of cell attachment and biofilm formation. This feature allowed us to track the giving up densities (GUDs) as a function of different initial prey densities (IPDs), something that is not possible in traditional microfluidic setups where the nutrient supply does not come from the substrate to which the cells attach (Fig. S2*B*). We observed that bacteria exhibit a detachment pattern where the ratio GUD/IPD remains approximately constant with changes in IPD (Figs. 2*E* and 3*A*). This type of response where the output to a given change in signal is inversely proportional to the signal background (here, IPD)—also known as Weber's law—occurs broadly in biological sensory systems, such as the chemotaxis signaling pathway of bacteria. Cells performing chemotaxis respond to the logarithm of the concentration gradient (therefore, rescaling the temporal gradient of concentration by the background concentration as in Weber's law) and adapt, within a broad concentration range (35), to the background concentration through the feedback provided by methylation of the chemoreceptors (36). Chemotaxis is a form of search strategy that is effective for nutrient fields under conditions of scalar symmetry (37) where the fields have the same pattern up to a multiplicative constant. For example, the diffusive process of tryptone from the agarose patch fulfills this requirement (Fig. 2*C*). The detachment response that we report (Fig. 3*A* and Fig. S8) has striking conceptual similarities with the chemotactic response. We speculate that the detachment response of *V. ordalii* shares several features of the chemotactic response, such as obeying Weber's law. This speculation is corroborated by the well-documented crosstalk between the chemotaxis pathway and the intracellular production of cyclic-di-GMP, which regulates the strength of cell attachment, and by the recent observation that cyclic-di-GMP acts upon the methylation state of the chemoreceptors (38). Particularly intriguing is the observation of the increased attachment propensity of bacterial cells upon starvation conditions, manifested in our study as an increased residence time on surfaces (Fig. 3*B*). The molecular characterization of this metabolism-dependent memory likely mediated by cyclic-di-GMP signaling, which impacts on bacterial motility and attachment dynamics, represents an exciting avenue of research.

Marine bacteria may be exposed to enhanced mortality risks while on a particle by predators, such as zooplankton, including copepods, flagellates, and ciliates, and by viral attack (39). Laboratory experiments and field observations (40) have documented that predators, including zooplankton, such as copepods, can localize, attach on, and ingest parts of a marine particle together with its associated bacteria (41). Copepods are able to detect and attack a marine particle by sensing and tracking the plume of dissolved organic matter in the wake of a sinking particle (42). This mechanism for finding particles suggests that larger and higher-quality particles, which generate larger and more intense plumes, will attract more predators. However, a study of the literature did not reveal direct evidence for any size dependence of this predation risk. Attached bacteria also suffer grazing mortality by attached flagellates and ciliates (43)—potentially a more important factor than the grazing pressure by copepods (39, 41). By combining modeling with experimental

measurements and observations of abundances of microbes on field-collected particles, the mortality rate of attached bacteria was estimated at 2.7 d^{-1} (disregarding viral attack) (43). The combined mortality rate of free-swimming bacteria must be on the same order of magnitude as their growth rate, which, for copiotrophs, such as *Vibrio ordalii*, is ∼1 d^{-1} in the ocean (44). This analysis suggests that the mortality risk is somewhat higher for attached than for free-living bacteria, although the statistical significance of this difference is currently impossible to quantify. With regard to viruses, literature indicates that the 100- to 1,000-fold higher concentrations of bacteria on particles (10^8–10^9 cells mL^{-1}) compared to the water column (10^5–10^6 cells mL^{-1}) are associated with higher densities of viruses on particles (45, 46). Because, on the one side, the encounter rate per bacterium is directly proportional to the concentration of viruses (24), this would suggest a higher per-bacterium rate of viral infection on particles. On the other side, the encounter rate per bacterium is directly proportional to the diffusion rate of both virus and bacterium (*SI Appendix*). The diffusion coefficient of the bacterium is drastically reduced while on a particle where the main source of diffusion for the bacterium is Brownian motion ($D_{BM} = 4 \times 10^{-13}$ m^2 s^{-1} for a bacterium), compared to the diffusion coefficient of a free-swimming bacterium ($D = 2 \times 10^{-10}$ m^2 s^{-1}). The effects on the encounter rate (and, therefore, on the infection rate by viral attack) of an increased concentration and a decreased diffusion coefficient for a bacterium attached to a particle seem to compensate each other. Again, however, a study of the literature did not reveal direct evidence for either higher per-bacterium viral infection rates on particles or any particle-size dependence of the viral infection risk. Our paper, thus, highlights the importance of measuring predation and viral infection risk on particles, ideally with explicit consideration of particle quality and particle size as bacteria may have additional strategies to further optimize their foraging in view of any enhanced risk of death as classically predicted by optimal foraging theory (47, 48).

The foraging strategies of marine bacteria, which structure bacteria–particle interactions and thus the fate of organic carbon in the ocean, have remained elusive, in part due to the difficulties of probing the behavioral ecology of marine microbes under naturally relevant conditions. By directly visualizing bacterial foraging in patchy microenvironments, we were able to apply and tailor patch use theory to microorganisms. Bacteria show evidence of conforming to predictions regarding patch use from OFT, yet bacterial foraging also presents significant differences compared to the foraging by metazoans for which patch use predictions were obtained. In patch use theory and its extensions, an animal is modeled as an independent forager randomly searching for prey in a patch (49) and possibly operating as a Bayesian forager (50). Bacteria are endowed with fundamentally different search and uptake mechanisms. They use chemoreceptors and uptake transporters distributed on the surface of the cell in combination with intracellular transduction pathways (22) to accurately measure the rates at which nutrient molecules reach their surface by molecular diffusion (51). Once they have attached to a surface, such as the agarose disk in our experiments, bacteria can accurately assess the diffusion-driven decrease of nutrient concentration over time at the surface of the patch without the need to move and sample the patch to evaluate local variations in patch quality (Movie S2) as is, instead, typical for a predator searching for prey within a patch. For the agarose-disk experiments since bacteria are randomly distributed on the surface of the patch (Fig. S5) in relatively low cell concentrations (Fig. 2*B*), each bacterium senses a very similar concentration, and thus bacteria can be modeled as single independent foragers. On marine particles, cell concentrations can become higher over time, causing either interference or synergistic effects (52, 53) that highlight the importance of extending patch use principles to account for cell aggregation. If allowance is made for the obvious physiological differences in sensory capabilities, ecological principles traditionally applied to animals—such as optimal foraging theory—can provide guidance and fundamental principles for the interpretation of microbial nutrient acquisition strategies and can represent a valuable framework to quantify and predict the role of marine bacteria in the uptake and cycling of nutrients in the ocean.

Materials and Methods

Bacterial Isolates and Cell Culture. The isolates and plasmids used in this study are listed in Table S1. Unless stated otherwise, all experiments used GFP-tagged *V. ordalii* 12B09. For routine culture, bacteria were grown in 1/2 strength 2216 medium (54) or on 2216 agar plates at 30 °C. An orbital shaker (600 rpm) was used for liquid cultures. For isolates harboring pGFP, spectinomycin (50 μg/mL) was added to maintain the plasmid.

Artificial Marine Particles Experiment. To study the behavior of bacteria toward marine particles in a model system (Fig. 1), we made particles consisting of agarose spheres loaded with tryptone and monitored the dynamics of attachment and detachment by bacteria. A stationary phase cell culture (optical density at 600 nm [OD_{600}] = 1.0) was washed with fresh medium, diluted to OD_{600} = 0.005 (7.0×10^6 CFU/mL), and then a 1-mL aliquot was introduced into a well of a 24-well microplate (Falcon). To mimic the dynamics of encounter with marine particles, four to five agarose spheres (∼500 μm in diameter) loaded with 0.1% tryptone (Difco) were released into the cell suspension at 25-min intervals. Particles were preincubated in 0.1% tryptone solution for >1 h and then released into the system by using a particle release device made in-house. To do this, particles were held on the tip of a custom particle holder, which was attached to a microscope condenser lens to allow precise vertical movement. The particle holder was made out of a plastic pipette tip, manufactured to have a crown- shaped tip with five points. Each point held an agarose sphere with the attachment being caused by the stickiness of the agarose spheres. By carefully lowering the condenser lens and, therefore, the tip of the particle holder to the air–water interface, particles were gently released into the liquid phase, detaching after contact with the air–water interface. The bacterial distribution over time (Fig. 1*A*) was visualized and recorded with a fluorescent microscope (Nikon, Eclipse Ti2) using a 4× objective (numerical aperture [N.A.] 0.13) and a scientific Complementary metal-oxide-semiconductor (sCMOS) camera (Andor Neo 5.5, 2,560 × 2,160 pixels). Cellular accumulation on the surface of the particles was quantified in terms of fluorescence intensity and measured with the NIS Elements software by setting a circular region of interest around each particle. To visualize simultaneously cellular attachment on the surface of a particle and chemoattractant diffusion (Fig. S1*D*), a 10× objective (N.A. 0.30) was used, and rhodamine B (20 μg/mL, Sigma-Aldrich) was employed as a diffusion proxy.

Agarose Patch Experiment. To allow visualization of the attachment and detachment of individual cells (Fig. 2) and thus enable measurement of the residence time, we carried out experiments using a 2D model particle consisting of an agarose disk (patch) containing tryptone. An agarose (3%-wt/vol) disk of diameter 3.8 mm and thickness 0.5 mm was placed within a recess of the same diameter created in a silicone gasket and fitted inside a 35-mm Petri dish (Falcon). The agarose disk was soaked in 0.2-, 1-, or 5-mM tryptone solution for 1 h prior to the experiments. A stationary phase cell culture (OD_{600} = 1.0) was washed with fresh medium, diluted to OD_{600} = 0.005 (7.0×10^6 CFU/mL), and then a 1-mL aliquot was introduced into the Petri dish to initiate the experiment. Cells attached to the upper surface of the patch were visualized and recorded with an inverted microscope (Nikon, Eclipse Ti2) using a 10× objective (N.A. 0.30) and a sCMOS camera (Andor Neo 5.5, 2,560 × 2,160 pixels). The number of cells on the agarose disk surface and their individual residence times were extracted from the video recordings using a custom MATLAB (The Mathworks, Natick, MA) cell-tracking routine.

Batch Surface Attachment Assays. The generality of the induction of the cellular attachment response of *V. ordalii* following the addition of tryptone was tested under a range of chemical conditions and in the presence of an inhibitor using batch surface attachment assays. A stationary phase cell culture (OD_{600} = 1.0) was washed with filtered autoclaved seawater, diluted to OD_{600} = 0.01 (1.5×10^7 CFU/mL), and then a 1-mL aliquot was introduced into a 35-mm Petri dish and incubated at 30 °C for 1 h. Test solutions (see below) were then added to determine the effect on bacterial attachment.

After removing planktonic cells by gently washing twice with filtered autoclaved seawater supplemented with tryptone (of the same concentration as the test solution in each trial), images of the bottom of the Petri dish at three locations were taken by phase contrast microscopy using a 4× objective (N.A. 0.13) and a sCMOS camera (Andor Neo 5.5, 2,560 × 2,160 pixels). Surface attachment was quantified by counting the attached cells using ImageJ. Three independent replicates were performed for each experiment. To determine the bacterial attachment kinetics, solutions of different concentrations of tryptone (at concentrations varying from 0 to 5 mM) were added to the cell suspension and the attachment response was quantified. The fraction of attached bacteria a, extracted from the attachment experiments as a function of the nutrient concentration C was fitted with Michaelis–Menten kinetics (Fig. 1*C*) $a(C) = a_{max}\, C/(C + K_A)$. The half-saturation constant $K_A = 0.35 \pm 0.08$ mM and the maximum number of attached bacteria a_{max} were extracted by performing a least squares minimization using Wolfram Mathematica v. 11.3 (Champaign, IL).

Effect of Starvation Period on Detachment Response. To determine whether *V. ordalii* adjusts its residence time in response to changes in the search time, we performed experiments in which we simulated a long search time by incubating cells for 3 h under starvation conditions in particle-free seawater, then compared their detachment behavior upon exposure to different concentrations of tryptone with the behavior of a control population that had not experienced a simulated long search time. Prior to the assays, cells were incubated for 3 h in unsupplemented seawater, while for the control experiment, cells were directly used after harvesting from the preculture (in tryptone-containing 2216 medium). The kinetics of detachment were analyzed by exposing the two cell populations to a high tryptone concentration, then quantifying the fraction of cells that underwent detachment after the concentration of tryptone was reduced (Fig. S6). A stationary-phase cell culture ($OD_{600} = 1.3$) was washed with filtered autoclaved seawater, diluted to $OD_{600} = 0.02$ (3×10^7 CFU/mL), and then a 1-mL aliquot was inoculated in a 35-mm Petri dish for 0.5 h to allow attachment under an initial concentration (IPD = 5 mM) of tryptone. After washing twice with fresh tryptone solution to remove planktonic cells, cells were exposed to an equal or lower concentration ($C = 5$, 1, 0.4, 0.1, 0.2, and 0 mM) of tryptone for 1.5 h, causing cells to undergo detachment. The numbers of attached cells before and after exposure to C were counted by imaging the lower surface of the Petri dish in phase contrast using a 20× objective (N.A. 0.45) with a sCMOS camera (Andor Neo 5.5, 2,560 × 2,160 pixels).

Growth Experiments. Growth rates of the bacteria under a range of resource concentrations were evaluated by measuring quasi-2D expansion of colonies (where the surface covered by the colonies is a proxy for the number of bacteria). A slab of 2216 agarose medium (agarose concentration = 3% wt/vol, 0.5-mm thick) was placed onto one of the wells of a 6-well plate, and colonies were allowed to form at the agarose–solid interface to facilitate inverted microscopy. Prior to experiments, the agarose slab was soaked in tryptone (at concentrations varying from 0 to 5 mM) and then inoculated with a dilute cell suspension. The experimental system was incubated at room temperature for 17 h on a microscope stage. Colonies were imaged in phase contrast at 20-min intervals using a 10× objective (N.A. 0.30) with a sCMOS camera (Andor Neo 5.5, 2,560 × 2,160 pixels). The 2D projected area of each colony was measured using a custom MATLAB image analysis routine.

Bacterial Growth Kinetics. The population growth rates extracted from the quasi-2D expansion of bacterial colonies for different tryptone concentrations (see *Growth Experiments*) were fitted with Michaelis–Menten kinetics (Fig. 1*C*). The half-saturation constant $K_G = 0.14 \pm 0.02$ mM and the maximum growth rate $r_{max} = 0.44 \pm 0.01$ h^{-1} were extracted by performing a least squares minimization using Wolfram Mathematica v. 11.3. The formula for the growth rate r as a function of the nutrient concentration C is $r(C) = r_{max}\, C/(C + K_G)$.

Data Availability. Bacterial attachment dynamics under different experimental conditions are available as Datasets S1–S3. All study data are included in the article and *SI Appendix*.

ACKNOWLEDGMENTS. We thank Thomas Kiørboe, Kay Bidle, Assaf Vardi, and two anonymous reviewers for useful comments, Vicente Fernandez and Bennett Lambert for discussions, Russell Naisbit for help with the editing of this paper, and Martin Polz for bacterial strains and plasmids. This work was supported by Gordon and Betty Moore Marine Microbial Initiative Investigator Award GBMF3783 (to R.S.), and Simons Foundation Grant 542395 (to R.S.) as part of the Principles of Microbial Ecosystems Collaborative (PriME).

1. F. Azam *et al*., The ecological role of water-column microbes in the sea. *Mar. Ecol. Prog. Ser.* **10**, 257–263 (1983).
2. S. W. Chisholm, Stirring times in the Southern ocean. *Nature* **407**, 685–687 (2000).
3. D. Bianchi, T. S. Weber, R. Kiko, C. Deutsch, Global niche of marine anaerobic metabolisms expanded by particle microenvironments. *Nat. Geosci.* **11**, 263–268 (2018).
4. G. A. Jackson, D. M. Checkley, Particle size distributions in the upper 100 m water column and their implications for animal feeding in the plankton. *Deep Sea Res. Part I Oceanogr. Res. Pap.* **58**, 283–297 (2011).
5. R. Kiko *et al*., Biological and physical influences on marine snowfall at the equator. *Nat. Geosci.* **10**, 852–858 (2017).
6. J. H. Martin, G. A. Knauer, D. M. Karl, W. W. Broenkow, Vertex: Carbon cycling in the Northeast Pacific. *Deep Sea Res. Part I: Oceanogr. Res. Pap.* **34**, 267–285 (1987).
7. F. Azam, F. Malfatti, Microbial structuring of marine ecosystems. *Nat. Rev. Microbiol.* **5**, 782–791 (2007).
8. D. E. Hunt *et al*., Resource partitioning and sympatric differentiation among closely related bacterioplankton. *Science* **320**, 1081–1085 (2008).
9. R. Stocker, Marine microbes see a sea of gradients. *Science* **338**, 628–633 (2012).
10. V. I. Fernandez, Y. Yawata, R. Stocker, A foraging Mandala for aquatic microorganisms. *ISME J.* **13**, 563–575 (2019).
11. E. L. Charnov, Optimal foraging, the marginal value theorem. *Theor. Popul. Biol.* **9**, 129–136 (1976).
12. L. M. Bautista, J. Tinbergen, A. Kacelnik, To walk or to fly? How birds choose among foraging modes. *Proc. Natl. Acad. Sci. U.S.A.* **98**, 1089–1094 (2001).
13. L. M. Bautista, J. Tinbergen, P. Wiersma, A. Kacelnik, Optimal foraging and beyond: How starlings cope with changes in food availability. *Am. Nat.* **152**, 543–561 (1998).
14. G. H. Pyke, Optimal foraging in hummingbirds–Testing the marginal value theorem. *Am. Zool.* **18**, 739–752 (1978).
15. P. Schmid-Hempel, A. Kacelnik, A. I. Houston, Honeybees maximize efficiency by not filling their crop. *Behav. Ecol. Sociobiol.* **17**, 61–66 (1985).
16. T. J. Wolf, P. Schmid-Hempel, Extra loads and foraging life-span in honeybee workers. *J. Anim. Ecol.* **58**, 943–954 (1989).
17. Y. Yawata *et al*., Competition-dispersal tradeoff ecologically differentiates recently speciated marine bacterioplankton populations. *Proc. Natl. Acad. Sci. U.S.A.* **111**, 5622–5627 (2014).
18. M. Valentini, A. Filloux, Biofilms and cyclic di-GMP (c-di-GMP) signaling: Lessons from *Pseudomonas aeruginosa* and other bacteria. *J. Biol. Chem.* **291**, 12547–12555 (2016).
19. H. Vlamakis, Y. Chai, P. Beauregard, R. Losick, R. Kolter, Sticking together: Building a biofilm the *Bacillus subtilis* way. *Nat. Rev. Microbiol.* **11**, 157–168 (2013).
20. O. X. Cordero *et al*., Ecological populations of bacteria act as socially cohesive units of antibiotic production and resistance. *Science* **337**, 1228–1231 (2012).
21. P. Raimbault, N. Garcia, F. Cerutti, Distribution of inorganic and organic nutrients in the South Pacific Ocean–Evidence for long-term accumulation of organic matter in nitrogen-depleted waters. *Biogeosciences* **5**, 281–298 (2008).
22. V. Sourjik, H. C. Berg, Receptor sensitivity in bacterial chemotaxis. *Proc. Natl. Acad. Sci. U.S.A.* **99**, 123–127 (2002).
23. J. Davis, R. Benner, Quantitative estimates of labile and semi-labile dissolved organic carbon in the western Arctic ocean: A molecular approach. *Limnol. Oceanogr.* **52**, 2434–2444 (2007).
24. T. Kiørboe, *A Mechanistic Approach to Plankton Ecology*, (Princeton University Press, Princeton, 2008).
25. L. Guidi *et al*., Relationship between particle size distribution and flux in the mesopelagic zone. *Deep Sea Res. Part I Oceanogr. Res. Pap.* **55**, 1364–1374 (2008).
26. S. Smriga, V. I. Fernandez, J. G. Mitchell, R. Stocker, Chemotaxis toward phytoplankton drives organic matter partitioning among marine bacteria. *Proc. Natl. Acad. Sci. U.S.A.* **113**, 1576–1581 (2016).
27. J. M. Pleasants, Optimal foraging by nectarivores–A test of the marginal-value theorem. *Am. Nat.* **134**, 51–71 (1989).
28. O. Olsson, J. S. Brown, Smart, smarter, smartest: Foraging information states and coexistence. *Oikos* **119**, 292–303 (2010).
29. C. Cozens-Roberts, J. A. Quinn, D. A. Lauffenburger, Receptor-mediated cell attachment and detachment kinetics. II. Experimental model studies with the radial-flow detachment assay. *Biophys. J.* **58**, 857–872 (1990).
30. T. Kiørboe, H. P. Grossart, H. Ploug, K. Tang, Mechanisms and rates of bacterial colonization of sinking aggregates. *Appl. Environ. Microbiol.* **68**, 3996–4006 (2002).
31. D. L. Kirchman, *Microbial Ecology of the Oceans*, (John Wiley & Sons Inc., Hoboken, N.J., ed. 2, 2008).
32. D. R. Brumley *et al*., Cutting through the noise: Bacterial chemotaxis in marine microenvironments. *Front. Mar. Sci.* **7**, 527, 10.3389/fmars.2020.00527 (2020).
33. C. K. Lee *et al*., Multigenerational memory and adaptive adhesion in early bacterial biofilm communities. *Proc. Natl. Acad. Sci. U.S.A.* **115**, 4471–4476 (2018).
34. C. Freitas, T. Glatter, S. Ringgaard, The release of a distinct cell type from swarm colonies facilitates dissemination of *Vibrio parahaemolyticus* in the environment. *ISME J.* **14**, 230–244 (2020).
35. T. S. Shimizu, Y. Tu, H. C. Berg, A modular gradient-sensing network for chemotaxis in *Escherichia coli* revealed by responses to time-varying stimuli. *Mol. Syst. Biol.* **6**, 382 (2010).
36. M. D. Lazova, T. Ahmed, D. Bellomo, R. Stocker, T. S. Shimizu, Response rescaling in bacterial chemotaxis. *Proc. Natl. Acad. Sci. U.S.A.* **108**, 13870–13875 (2011).
37. O. Shoval *et al*., Fold-change detection and scalar symmetry of sensory input fields. *Proc. Natl. Acad. Sci. U.S.A.* **107**, 15995–16000 (2010).

38. L. Xu *et al.*, A cyclic di-GMP-binding adaptor protein interacts with a chemotaxis methyltransferase to control flagellar motor switching. *Sci. Signal.* **9**, ra102 (2016).
39. J. Pernthaler, Predation on prokaryotes in the water column and its ecological implications. *Nat. Rev. Microbiol.* **3**, 537–546 (2005).
40. K. O. Moller *et al.*, Marine snow, zooplankton and thin layers: Indications of a trophic link from small-scale sampling with the video plankton recorder. *Mar. Ecol. Prog. Ser.* **468**, 57–69 (2012).
41. T. Kiørboe, How zooplankton feed: Mechanisms, traits and trade-offs. *Biol. Rev. Camb. Philos. Soc.* **86**, 311–339 (2011).
42. F. Lombard, M. Koski, T. Kiorboe, Copepods use chemical trails to find sinking marine snow aggregates. *Limnol. Oceanogr.* **58**, 185–192 (2013).
43. T. Kiørboe, K. Tang, H. P. Grossart, H. Ploug, Dynamics of microbial communities on marine snow aggregates: Colonization, growth, detachment, and grazing mortality of attached bacteria. *Appl. Environ. Microbiol.* **69**, 3036–3047 (2003).
44. D. L. Kirchman, Growth rates of microbes in the oceans. *Annu. Rev. Mar. Sci.* **8**, 285–309 (2016).
45. M. G. Weinbauer *et al.*, Viral ecology of organic and inorganic particles in aquatic systems: Avenues for further research. *Aquat. Microb. Ecol.* **57**, 321–341 (2009).
46. C. H. Wigington *et al.*, Re-examination of the relationship between marine virus and microbial cell abundances. *Nat. Microbiol.* **1**, 15024 (2016).
47. J. S. Brown, Patch use as an indicator of habitat preference, predation risk, and competition. *Behav. Ecol. Sociobiol.* **22**, 37–47 (1988).
48. C. W. Clark, Antipredator behavior and the asset-protection principle. *Behav. Ecol.* **5**, 159–170 (1994).
49. J. S. Brown, Patch use under predation risk. 1. Models and predictions. *Ann. Zool. Fenn.* **29**, 301–309 (1992).
50. O. Olsson, J. S. Brown, H. G. Smith, Gain curves in depletable food patches: A test of five models with European starlings. *Evol. Ecol. Res.* **3**, 285–310 (2001).
51. H. C. Berg, E. M. Purcell, Physics of chemoreception. *Biophys. J.* **20**, 193–219 (1977).
52. A. Ebrahimi, J. Schwartzman, O. X. Cordero, Cooperation and spatial self-organization determine rate and efficiency of particulate organic matter degradation in marine bacteria. *Proc. Natl. Acad. Sci. U.S.A.* **116**, 23309–23316 (2019).
53. H. Jeckel *et al.*, Learning the space-time phase diagram of bacterial swarm expansion. *Proc. Natl. Acad. Sci. U.S.A.* **116**, 1489–1494 (2019).
54. C. E. Zobell, Studies on marine bacteria. 1. The cultural requirements of heterotrophic aerobes. *J. Mar. Res.* **4**, 42–75 (1941).